Nanostructures and Oxidation Kinetics of Diesel Particulate Matters

Preechar Karin[*1], Hiroshi Oki[2], Katsunori Hanamura[2] and Chinda Charoenphonphanich[3]

[1] International College, King Mongkut's Institute of Technology Ladkrabang, Bangkok, Thailand 10520
[2] Faculty of Mechanical and Control Engineering, Tokyo Institute of Technology, Tokyo, Japan 152-8552
[3] Faculty of Engineering, King Mongkut's Institute of Technology Ladkrabang, Bangkok, Thailand 10520
* Corresponding Author: Tel: 02 329 8261-2, Fax: 02 737 2580,
E-mail: kkpreech@kmitl.ac.th

Abstract

Diesel particulate matters (PMs) must be removed from the exhaust gas emitted from diesel engines to protect the environment and human health; therefore, regulation of vehicle emissions has become increasingly strict. The nanostructures of diesel particulate matters emitted from an actual diesel engine and a diffusion flame burner were investigated by using a transmission electron microscopy (TEM) for better understanding. The single particulate's sizes of both engine and burner were approximately 20-80 nm. The various size of particulate might be strongly related to drag and shear forces of fluid flow, Brownian motion force of gases molecules and electrostatic forces of charges carbon elements, even though such forces is the order of Pico-Newton. Thermo-gravimetric analysis (TGA) was used to investigate chemical kinetics of PM oxidation. The apparent activation energies of engine's PM oxidation were approximately 105kJ/mol and 248kJ/mol for hydrocarbon and carbon zones, respectively. On the other hand, the apparent activation energies of lamp's PM oxidation were approximately 139kJ/mol and 218kJ/mol, respectively. Consequently, much amount of soluble organic fraction (SOF) emitted from an actual engine may be strongly affected to the low apparent activation energy at the low temperature oxidation zone. Similarly, an internal combustion engine operates with very high temperature and pressure. Structure of soot emitted from diesel engine may be strong carbon bonding resulting in increasing of the apparent activation energy of carbon oxidation.

Keywords*:* Diesel particulate matter, Diesel particulate filter, Hydrocarbon, Apparent activation energy.

1. Introduction

Among internal combustion engines, diesel engines have the highest thermal efficiency. However, particulate matters (PMs) must be removed from exhaust gases that are emitted by diesel engines to protect the environment and human health. Diesel particulate matters consist of a solid fraction (SOL) and a soluble organic fraction (SOF). Primary particles, composed of carbon and metallic ash, are coated with SOF and sulfate. The mean diameter of the primary and

agglomerated particles is usually in the range of 20–80 nm and 80–300 nm, respectively. The composition of particles from a diesel engine may vary widely depending on the operating conditions and fuel composition [1–5].

The nanostructures of primary soot particles have been characterized using transmission electron microscopy (TEM) to understand them in detail. A primary soot particle has two distinct parts: an inner core and an outer shell. The inner core has a diameter of 10 nm and it is located at the central region of the primary particle [6, 7].

The electric charge of carbon particles sampled from combustion flames and diesel engines have also been reported. Carbon particles in the later stage of growth are assumed to be charged by thermionic emission and electron capture. The number of charges per particle is varies but average is two. The potential energy increases with increasing charge when the radius of the soot particle is fixed, and decreases with increasing radius for a constant charge [8, 9].

Diesel particulate filters (DPFs) play an important role in particulate trapping and oxidation (regeneration of DPFs). A DPF is generally made of ceramic materials, such as cordierite or silicon carbide, consisting of many rectangular channels with alternate channels blocked using cement at each end. The exhaust gas is forced to flow through a channel wall having numerous micron-scale pores that trap the PM. Furthermore, the collected PM must be oxidized to regenerate the DPF and reduce the back pressure on the diesel engine. A number of studies have been performed to simulate particulate trapping and chemical reactions inside DPFs and provide valuable information in designing them [10–14].

Catalytic fuel additives and catalyst DPFs have been proven to reduce the overall activation energy required for particulate oxidation, resulting in lower-temperature oxidation compared to non-catalyst DPFs [15, 16]. The oxidation reaction of soot has been investigated using thermogravimetric analysis (TGA) and temperature program oxidation (TPO) to evaluate catalytic activities [17–20]. Moreover, the oxidation of soot on conventional and under developing DPFs were also reported [21-23].

Although structure and oxidation of particulate involve complex behaviors, very few information is available to aid in understanding such phenomena. In the present study, micro-, nano-structures and oxidation behaviors are investigated by using TEM and TGA to aid in better understanding and future designing of an ideal DPF configuration.

2. Experimental Procedure

Figure 1 shows an experimental procedure of nano-structures and oxidation behaviors are investigated by using TEM and TGA. A diesel fuel lamp (conventional diesel fuel of JIS K2204 No. 2) was used in the soot generation process. Part of the soot inside the diesel flame was introduced into PM collector through a bypass line. Similarly, a diesel engine (Robin SDG2200, manufactured by Subaru Co. Ltd.) with a displacement of 230 cm^3 and a rated output of 2.8 kW was also used in the soot generation

process. The fuel injection pressure was approximately 50 MPa. The engine was operated under a constant load of 2.0 kW at a constant speed of 3000 rpm throughout the experiment. Finally, particulate of each group are investigate by TEM, TGA and CHN. For the thermal and oxidation analysis of oxidizable particulates, the operating conditions are as follow: temperature increases at a rate of 10 $^{\circ}$C per minute from 15 $^{\circ}$C to 700 $^{\circ}$C with oxygen of 10% and nitrogen of 90% atmosphere.

Lamp ➡ PM collector ➡ TEM, TGA, CHN

Engine ➡ PM collector ➡ TEM, TGA, CHN

Fig. 1 Particulate emitted from a lamp and an engine are captured for characterization.

3. Results and Discussion

3.1 Structure of PM

Figure 2a and 2b shows TEM images of diesel particulates emitted by the diesel fuel lamp and the diesel engine, respectively. The uniform size of primary (single) of ultrafine particulates can be clearly seen. The single particulate's sizes of both engine and lamp were approximately 20-80 nm. Nanostructures such as density of crystallite and length of each crystallite of pure carbon inside diesel lamp and diesel engine PMs are very similar, as shown in Fig.3a (diesel lamp) and 3b (diesel engine). Figure 4a shows TEM image of homogenous carbon crystallite. The crystallite of carbon was approximately 3–5 nm × 1 nm in length and thickness, respectively. A crystallite of carbon consists of approximately 3,000 atoms. A single particle of PM contains approximately 0.1 to 10 million atoms. A primary soot particle has two distinct parts: an inner core and an outer shell. The inner core has a diameter of 10 nm and it is located at the central region of the primary particle. The size of each crystallite and agglomeration of many crystallites and size of Primary particle might be strongly related to Brownian force of gas molecule, drag

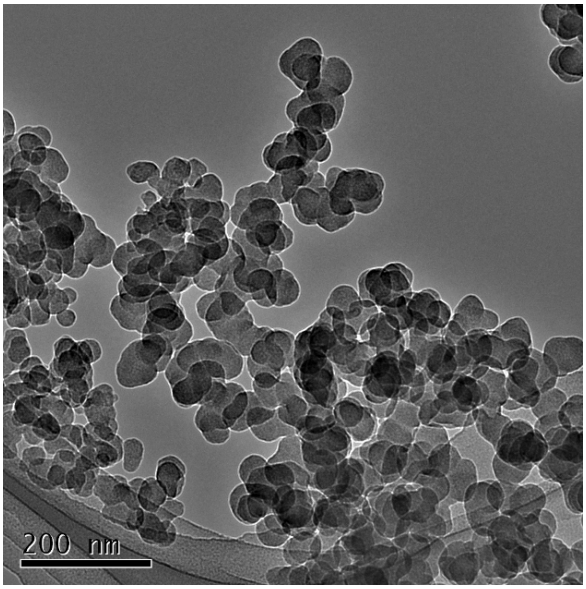

(a)

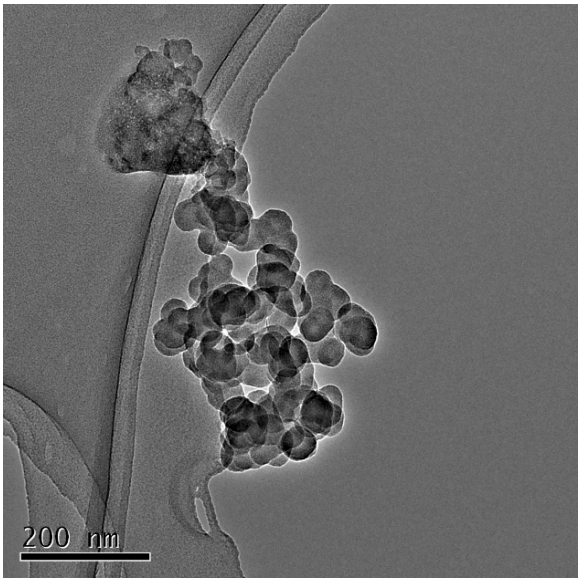

(b)

Fig. 2 TEM images of (a) lamp and (b) engine diesel fine particles (accumulate) of PMs.

and shear forces of fluid dynamics, electrostatics forces of charge elements.

Moreover, some soot was agglomerated with ash (calcium), which included in lubricant oil, as shown in Fig.2b. It was clearly observed the different nanostructure of carbon and

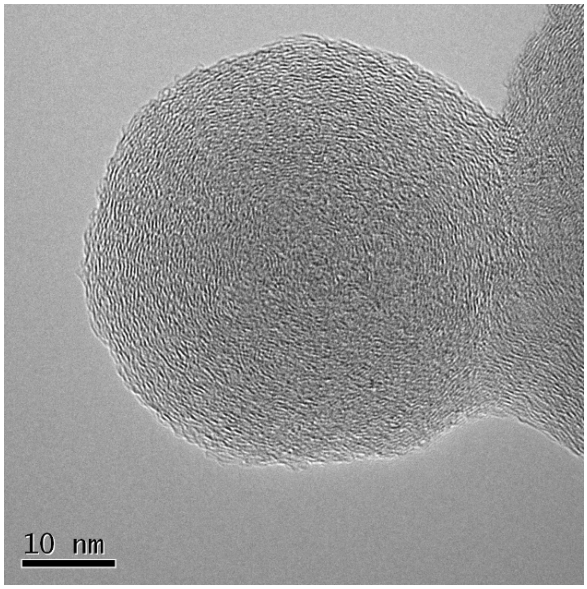

(a)

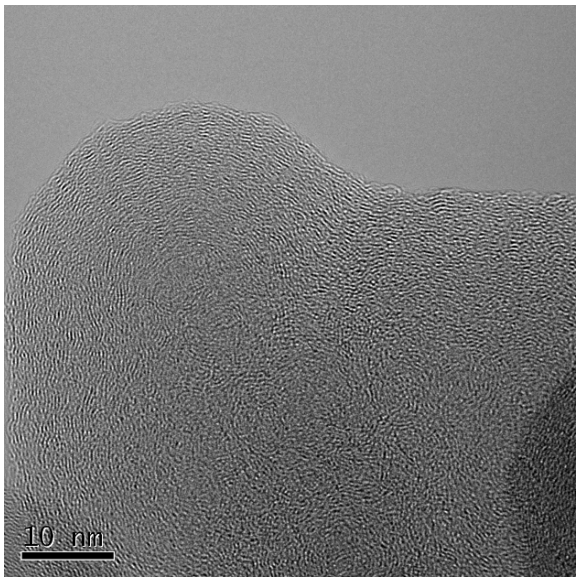

(b) [23]

Fig. 3 TEM images of (a) lamp and (b) engine diesel ultra fine particles (primary) of PMs.

calcium. The pattern of carbon crystallite looks like a curve line (4a), where as the pattern of ash crystallite looks like a straight cross line (4b). Generally, ash is unburned additives of fuel itself and engine lubrication oil.

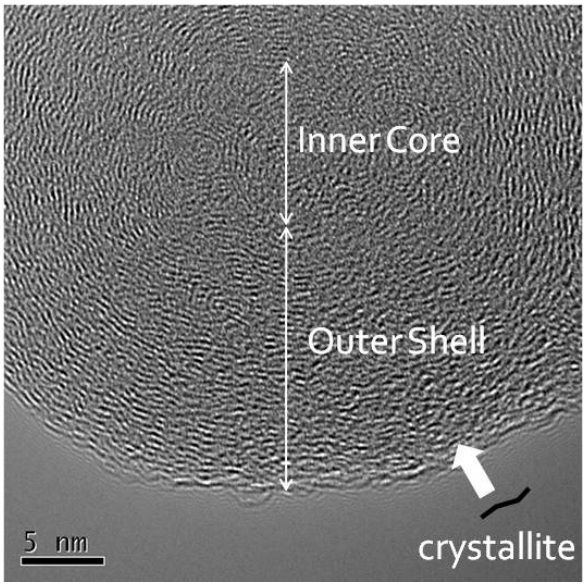

(a)

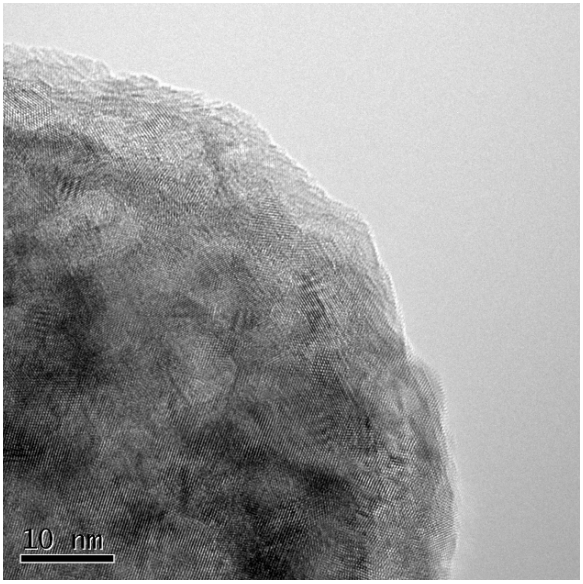

(b)

Fig. 4 TEM images of (a) carbon (soot) and (b) ash nanostructures of PMs.

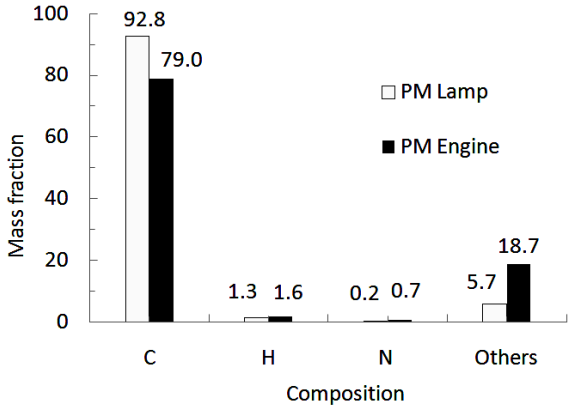

Fig. 5 Compositions of particulate using CHN (Carbon Hydrogen Nitrogen) gas analysis.

3.2 Composition of PM

The composition of each PM was characterized by CHN analyzer (oxidized gas analysis) for better understanding. The amount of unburned HC was estimated by using CHN analyzer during oxidation of PM emitted from the diesel engine compared to that on the diesel fuel lamp, as shown in Fig. 5. The mass fraction of C, H, N and others (ash, sulfate etc.) inside PMs were converted from gas analysis during combustion. The mass fraction of C inside PM emitted from the diesel engine smaller than that from the diesel fuel lamp, whereas the mass fraction of H and ash were largest. As a result, particulate emitted by the diesel engine might be composed of largest amount of adsorbed SOF compared to that by the diesel lamp. Moreover, much amount of other composition (ash, sulfate etc.) on particulate emitted from the diesel engine was also observed.

3.3 Oxidation of PM

In order to investigate the reaction behavior of each PM, a comparison between activation energies for reactions of diesel lamp's particulates and diesel engine's particulates was made, where the activation energy was obtained from the reduction rates of PM mass and the DPF temperature. Here, the particulates were assumed to be reacted with oxygen and resulted in products of CO and CO_2 as follows:

$$PMs + O_2 \rightarrow CO + CO_2 \quad (1)$$

The reduction rate of particulates moles can be expressed as follows:

$$-\frac{d[Y]}{dt} = -k[Y]^n[O_2]^m \quad (2)$$

Here, [*Y*] is the remaining moles of carbon at each time step during regeneration. The reaction coefficient *k* can be described by the Arrhenius-type reaction rate expression. As a result, the activation energy is obtained as the gradient of the following equation:

$$\ln\left[\frac{-1}{[Y]^n}\frac{d[Y]}{dt}\right] = -\frac{E}{RT} + (\ln A + m\ln[O_2]) \quad (3)$$

Here, *E* is the activation energy, *A* is the frequency factor, *R* is the gas constant, *T* is the absolute temperature of the DPF, and the last term on the right-hand side in Eq.(3) is assumed to be constant. The above reaction was independent of any value of reaction order, *n*, in the range between 2/3 of the shrinking core model and 1. In this study, the reaction order *n* was assumed to be 1 for simplicity [21-23].

The mass conversion during oxidation of their oxidizable PM was also analyzed using the TGA. Figures 6a and 6b show the particulate mass conversion and conversion rate, respectively, with respect to time. The mass of particulate emitted from the diesel engine decreased faster than that from the diesel fuel lamp. There are two peak of mass decreasing rate for PM emitted from the diesel engine, whereas, only one peak of PM mass decreasing rate for the diesel fuel lamp—which very high purity of carbon compared to that on the diesel engine.

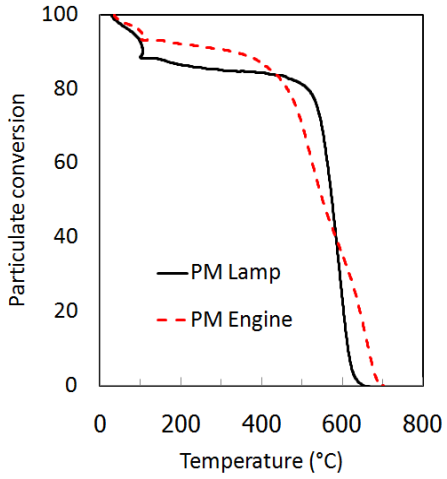

(a)

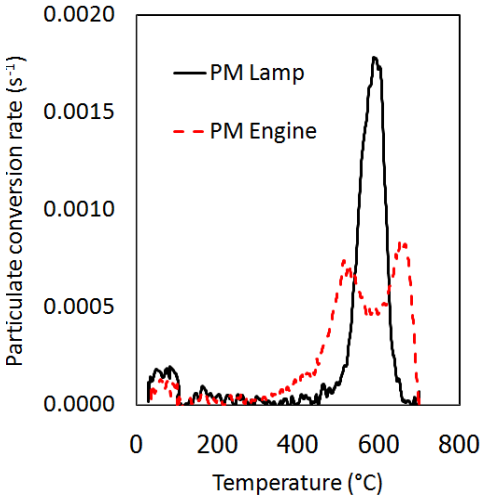

(b)

Fig. 6 (a) Particulate conversion and (b) particulate conversion rate by TGA.

The particulate conversion curves may be divided into three regions. In the first region, from 50 °C to 100 °C, it can be considered the evaporation of water molecules. In the second region, from 100 °C to 450 °C, that is assumed to be hydrocarbon oxidation. In the third region, from 450 °C to 700 °C, that is assumed to be carbon oxidation. In this region, the weight of particulate is decreased larger than that of moisture and hydrocarbon regions.

Figure 7a shows the Arrhenius plots used to obtain the apparent activation energy for the lamp's PM oxidation. The Arrhenius plots of PM emitted from the lamp may be divided into two regions. In the first region, as shows in the temperature of 425 to 515 °C, the activation energy is 139.4 kJ/mol. It can attribute to the reaction between strong bonding of hydrocarbon and oxygen. In the second region, shows as the temperature above 515 °C, the activation energy is 218.9 kJ/mol. It can attribute to the reaction between carbon and oxygen.

Figure 7b shows the Arrhenius plots used to obtain the apparent activation energy for the engine's PM oxidation. The Arrhenius plots of PM emitted from the engine may be divided into three regions. In the first region, as shows in the temperature lower than 425 °C, the activation energy is 48.5 kJ/mol. In the second region, shows as the temperature between 425 to 515 °C, the activation energy is 104.9 kJ/mol. It can attribute to the oxidation of very weak hydrocarbon (unburned fuel) and weak

hydrocarbon in the first and second regions, respectively. In the third region, as shown in the temperature above 515 °C, the activation energy is 248.3 kJ/mol. It can attribute to the oxidation of very strong carbon. Table 1 summarizes the apparent activation energy of each PM oxidation.

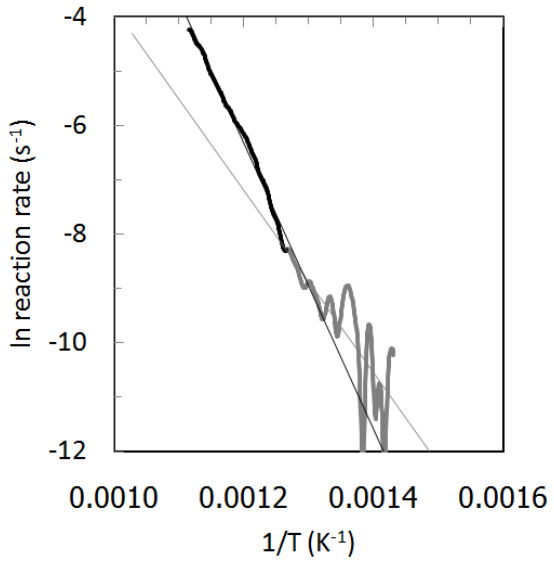

(a)

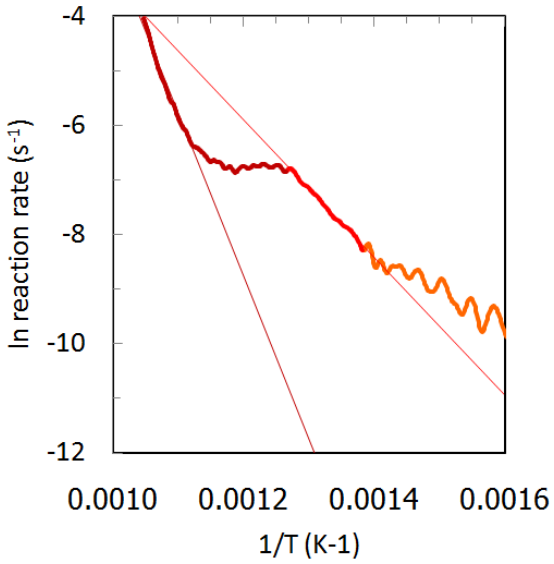

(b)

Fig. 7 Arrhenius plot of (a) particulates emitted by (a) lamp and (b) engine.

Table 1 Apparent activation energy calculated from oxidation rate of each PM.

PM	E_a (kJ/mol)		
Type	<425 °C	425-515 °C	>515 °C
Lamp	-	139.4	218.9
Engine	48.5	104.9	248.3

4. Conclusion

1. Nanostructures of pure carbon inside diesel lamp and diesel engine PMs are very similar, even though, some part of soot was agglomerated with ash, which included in lubricant oil of diesel engine.

2. The mass fraction of carbon inside PM emitted from the diesel engine is smaller than that from the diesel fuel lamp, whereas the mass fraction of H was largest. As a result, particulate emitted by the diesel engine might be composed of largest amount of adsorbed SOF compared to that by the low temperature and pressure of diesel lamp diffusion flame.

3. Soluble organic fraction (SOF) emitted from an actual engine (incomplete combustion) might strongly affected the low temperature oxidation zone resulting in low apparent activation energy.

4. The strong carbon bonding of engine soot (high temperature and pressure operation) might strongly cause the oxidation apparent activation energy higher than that of lamp soot (low flame temperature and pressure).

5. Acknowledgement

The authors gratefully acknowledge support from Isuzu Research Center and NGK Insulator.

6. References

[1] Heywood, J.B. (1998). Internal Combustion Engine Fundamental, McGraw-Hill series in mechanical engineering, Singapore.

[2] Smith, O.I. (1981). Fundamentals of soot formation in flames with application to diesel engine particulate emissions, *Progress in Energy and Combustion Science*, Vol. 7, pp.275-291.

[3] Maricq, M.M. (2007). Review Chemical Characterization of particulate emissions from diesel engine: A review, *Journal of Aerosol Science*, Vol.38, pp.1079-1118.

[4] Kittelson, D.B. (1998). Engines and nanoparticles: A review, *Journal of Aerosol Science*, Vol.29, pp.575-588.

[5] Majewski, W.A. and Khair, M.K. (2006). Diesel Emissions and Their Control, SAE Order No.R-303, SAE International. Warrendale USA.

[6] Ishiguro, T. Takatori, Y. and Akihama, K. (1997). Microstructure of Diesel Soot Particles Probed by Electron Microscopy: First Observation of Inner Core and Outer Shell, *Combustion and Flame*, 108, pp.231-234.

[7] Vander Wal, R.A. Yezerets, A. Currier, N.W. Kim, D.H. and Wang, C.H. (2007). HRTEM Study of diesel soot collected from diesel particulate filters, *Carbon*, 45, pp.70-77.

[8] Ball, R.T. and Howard, J.B. (1971). Electric charge of carbon particles in flames, *Symposium (International) on Combustion*, Vol.13, Issue 1, pp.353-362.

[9] Maricq, M.M. (2006). On the electrical charge of motor vehicle exhaust particles, *Journal of Aerosol Science,* Vol.37, pp.858-874.

[10] Konstandopoulos, A.G. Kostoglou, M. Vlachos, N. and Kladopoulos, E. (2005). Progress in Diesel Particulate Filter Simulation, *SAE Technical paper*, 2005-01-0946.

[11] Konstandopoulos, K.G. Zarvalis, D. Kladopoulou E. and Dolios, L. (2006). A multi-reactor assembly for screening of diesel particulate filters, *SAE Technical paper*, 2006-01-0874.

[12] Tushima, S. Nakamura, I. Sakashita, S. Hirai, S. and Kitayama, D. (2010). Lattice Boltzmann simulation on particle transport and captured behaviors in a 3d-reconstructed micro porous DPF, *SAE Technical paper*, 2010-01-0534.

[13] Hanamura, K. Karin, P. Cui, L. Rubio, P. Tsuruta, T. Tanaka, T. and Suzuki, T. (2009). Micro- and macroscopic visualization of particulate matter trapping and regeneration processes in wall-flow diesel particulate filters, *International Journal of Engine research*, Professional Engineering Publishing, Vol.10, No.5/2009, pp.305-321.

[14] Karin, P. Cui, L. Rubio, P. Tsuruta, T and Hanamura, K. (2009). Microscopic Visualization of PM Trapping and Regeneration in Micro-Structural Pores of a DPF Wall, *SAE International Journal of Fuels and Lubricants,* SAE International, Vol.2, No.1, pp.661-669.

[15] Fino, D. and Specchai, V. (2008). Review open issues in oxidative catalysis for diesel particulate abatement, *Powder technology*, Vol.180, pp.64-73.

[16] Suzuki, J. and Matsumoto, S. (2004). Development of catalysts for diesel particulate NOx reduction, *Topics in Catalyst*, Vol.28, pp.171-176.

[17] Neeft, J.P.A. Nijhuis, T.X. Smakman, E. Makkee, M. and Moulijn, J.A. (1997). Kinetics of the oxidation of diesel soot, *Fuel*, Vol.76, No.12, pp.1129-1136.

[18] Darcy, P. Costa, P.D. Mellottee, H. Trichard J.M. and Mariadassou, G.D. (2007). Kinetics of catalyzed and non-catalyzed oxidation of soot form a diesel engine, *Catalysis Today*, Vol.119, pp.252-256.

[19] Yezerets, A. Currier, N.W. and Eadler, H.A. (2003). Experimental Determination of the Kinetics of Diesel Soot Oxidation by O_2 – Modeling Consequences, *SAE Technical paper*, 2003-01-0833

[20] Lorentzou, S. Pagkoura, C. Zygogianni, A. Kastrinaki, G. and Konstandopoulos, A.G. (2008). Catalytic nano-structured materials for next generation diesel particulate filters, *SAE Technical paper*, 2008-01-0417.

[21] Karin, P. and Hanamura, K. (2010). Particulate Matter Trapping and Oxidation on Catalyst-Membrane, *SAE International Journal of Fuels and Lubricants,* SAE International, Vol.3, No.1, pp.368-379.

[22] Karin, P. and Hanamura, K. (2010). Particulate Matter Trapping and Oxidation on a Diesel Particulate Filter, *The First TSME International Conference on Mechanical Engineering,* 2010.

[23] Oki, H. Karin, P. and Hanamura, K. (2010). Visualization of Oxidation of Soot Nanoparticles Trapped on a Diesel Particulate Membrane Filter, *SAE International Journal of Engine,* SAE International, 2011-01-0602.